Appendix

Vibrational state densities for cyclopentene, 1-methylcyclopentene, and vinylcyclopropane were computed from harmonic oscillator models by exact count.[19] Fundamental vibrational wavenumbers used were: cyclopentene,[3] 3070, 3068, 2963, 2938, 2933, 2903, 2882, 2860, 1617, 1473, 1448, 1438, 1353, 1302, 1268, 1209, 1207, 1134, 1128, 1109, 1047(2), 1037, 962, 933, 896, 879, 695(2), 600, 593, 390, 127; 1-methylcyclopentene,[45] 3052, 2966, 2960, 2955, 2936, 2924, 2903, 2868, 2863, 2858, 1662, 1474, 1456, 1446, 1436, 1383, 1335, 1299, 1261, 1218, 1203, 1149, 1135, 1064, 1032, 1009, 1006, 928, 906, 888, 879, 873, 858, 817, 788, 642, 574, 432, 330, 228, 170, 104; vinylcyclopropane,[17] 3050 (8), 1625, 1425 (3), 1300 (20), 1050 (2), 1000 (8), 900, 800 (2), 425, 310 (2), 50. In methylcyclopropane and vinylcyclopropane the methyl and vinyl groups were treated as torsional vibrations of 170 and 50 cm^{-1}, respectively.

Registry No. Cyclopentene, 142-29-0; cyclopentadiene, 542-92-7; 1,4-pentadiene, 591-93-5; *cis*-1,3-pentadiene, 1574-41-0; *trans*-1,3-pentadiene, 2004-70-8; 1-methylcyclopentene, 693-89-0; vinylcyclopropane, 693-86-7.

Electronic Spectra from Molecular Dynamics: A Simple Approach

John P. Bergsma, Peter H. Berens, Kent R. Wilson,*

Department of Chemistry, University of California, San Diego, La Jolla, California 92093

Donald R. Fredkin,

Department of Physics, University of California, San Diego, La Jolla, California 92093

and Eric J. Heller

Theoretical Division, T-12, Los Alamos National Laboratory, Los Alamos, New Mexico 87545
(Received: August 12, 1983)

A method is illustrated for computing the contours of electronic absorption bands from classical equilibrium or nonequilibrium molecular dynamics (or equally for equilibrium systems from Monte Carlo or explicit integration over coordinates). The inputs to the calculations are the potential energy curves for the different electronic states and the electronic transition dipole moments between the states as functions of nuclear coordinates. A simple quantum correction by temperature scaling is demonstrated for the thermal equilibrium case. A test is carried out for the I_2 visible absorption spectrum involving transitions from the ground X $0_g^+(^1\Sigma)$ to the excited A $1_u(^3\Pi)$, B $0_u^+(^3\Pi)$ and B'' $1_u(^1\Pi)$ states, for thermal equilibrium gas-phase I_2. The electronic band contours are computed and shown to be remarkably similar to the measured contours. This method and others such as the methods of Lax, Lee, Tellinghuisen, and Moeller and the Landau–Zener–Stuckleberg–Tully–Preston surface hopping approach are shown all to be mutually equivalent, while the usual reflection method is shown to be related but nonequivalent.

I. Introduction

In this paper we show how molecular dynamics can be used in a simple manner to compute the contours of electronic absorption bands. The motivation for this work is to compute transient electronic spectra for many atom systems.[1,2] We could equally use Monte Carlo or explicit integration over coordinates to compute equilibrium electronic absorption bands. However, molecular dynamics provides the only means to calculate these band contours in a nonequilibrium system. Thus, by demonstrating that molecular dynamics yields the correct absorption band contour for the equilibrium case, we can justify using this technique in the nonequilibrium case. We have already elsewhere[1,2] applied the methods derived in this paper to the calculation of the transient electronic absorption spectra from a chemical reaction occurring in solution. In another paper[3] the electronic absorption spectrum for an initially thermal equilibrium system is computed by a time-dependent wave packet technique, and the result for the same I_2 molecular test case can be compared to the more classical technique developed here.

In section II we discuss the theory which we will use, as well as a harmonic quantum correction appropriate for thermal equilibrium. Section III contains a comparison with other semiclassical approaches for electronic spectra. The potential energy and electronic transition dipole vs. internuclear distance functions used to compute the sample I_2 visible absorption band contours are presented in section IV. Section V discusses the computational

(1) P. Bado, P. H. Berens, J. P. Bergsma, S. B. Wilson, K. R. Wilson, and E. J. Heller in "Picosecond Phenomena", Vol. III, K. B Eisenthal, R. M. Hochstrasser, W. Kaiser, and A. Laubereau, Ed., Springer-Verlag, Berlin, 1982, p 260.

(2) P. Bado, P. H. Berens, J. P. Bergsma, M. H. Coladonato, C. G. Dupuy, P. M. Edelsten, J. D. Kahn, K. R. Wilson, and D. R. Fredkin in "Proceedings of the International Conference on Photochemistry and Photobiology", A. Zewail, Ed., Harwood Academic, New York, in press.

(3) J. R. Reimers, K. R. Wilson, and E. J. Heller, *J. Chem. Phys.*, in press.

0022-3654/84/2088-0612$01.50/0

method and section VI compares calculated and measured equilibrium I_2 gas-phase band contours. Finally, in section VII we discuss the results and their significance.

II. Theory

A. Absorption Cross Section. The absorption cross section $\sigma(\omega)$ can be expressed in the usual first-order time-dependent perturbation theory approach as[4-6]

$$\sigma(\omega) = \frac{4\pi^2\omega}{\hbar cn}\sum_{i,f}(\rho_i - \rho_f)|\langle f|\hat{\epsilon}\cdot\mu|i\rangle|^2\,\delta(\omega_{fi} - \omega) \qquad (2.1)$$

in which ω is the angular frequency, $\hbar$ is Planck's constant divided by 2π, c is the speed of light, n is the index of refraction, ρ_i and ρ_f are the probabilities in the ensemble of initial and final states, $\langle f|$ is a final state, $|i\rangle$ an initial state, $\hat{\epsilon}$ is a unit vector in the direction of the electric field of the probe light, μ is the electric dipole operator

$$\mu = \sum_j q_j \mathbf{r}_j \qquad (2.2)$$

in which q_j is the charge and $\mathbf{r}_j$ the position of the jth particle, and the argument to the Dirac δ function is in terms of the angular frequency difference

$$\omega_{fi} = (E_f - E_i)/\hbar \qquad (2.3)$$

between the energies E_f and E_i of the final and initial states.

For an equilibrium system

$$\rho_i - \rho_f = \rho_i(1 - e^{-\beta\hbar\omega}) \qquad (2.4)$$

where $\beta = (k_B T)^{-1}$ in which k_B is Boltzmann's constant and T the temperature. We use the usual linear response[4-6] conversion to the Heisenberg picture and closure to write

$$\sigma(\omega) = \frac{4\pi^2\omega[1 - e^{-\beta\hbar\omega}]}{\hbar cn}(2\pi)^{-1}\int_{-\infty}^{\infty} dt\, e^{-i\omega t}\sum_i \rho_i\langle i|[\hat{\epsilon}\cdot\mu(0)][\hat{\epsilon}\cdot\mu(t)]|i\rangle \qquad (2.5)$$

in which $\mu(0)$ and $\mu(t)$ are the Heisenberg time-dependent dipole moment operators evaluated at times 0 and t. If we adopt a classical picture for the dipole moment $\mu(t)$, we may rewrite[6] eq 2.5 in terms of the spectral density operator D as

$$\sigma(\omega) = \frac{4\pi^2\omega[1 - e^{-\beta\hbar\omega})}{\hbar cn}\langle D[\hat{\epsilon}\cdot\mu]\rangle \qquad (2.6)$$

in which $\langle\rangle$ indicates an ensemble average over initial states (a thermal average for the equilibrium case) and the spectral density operator per unit angular frequency is defined as

$$D[f] \equiv D[f,f] = (2\pi)^{-1}\lim_{\tau\to\infty}\frac{1}{2\tau}\int_{-\tau}^{\tau} dt\, e^{-i\omega t}\, f(t)\int_{-\tau}^{\tau} dt'\, e^{i\omega t'}\, f^*(t') \qquad (2.7a)$$

$$= (2\pi)^{-1}\lim_{\tau\to\infty}\frac{1}{2\tau}\left|\int_{-\tau}^{\tau} dt\, e^{-i\omega t}\, f(t)\right|^2 \qquad (2.7b)$$

For a nonequilibrium system there is no a priori relationship between ρ_i and ρ_f. We will assume here for nonequilibrium systems that $\rho_f \approx 0$. This means, for example, that we may start with a small density of final states and illuminate weakly enough so that the final states are not pumped appreciably. The appropriate linear response relationship is then

$$\sigma(\omega) = \frac{4\pi^2\omega}{\hbar cn}\langle D[\hat{\epsilon}\cdot\mu]\rangle \qquad (2.8)$$

in which $\langle\rangle$ now indicates an average over a nonequilibrium ensemble.

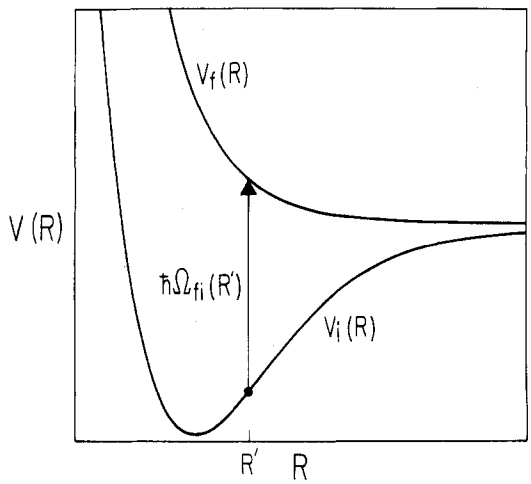

Figure 1. Diagram illustrating the angular frequency $\Omega_{fi}(R') = \hbar^{-1}\cdot[V_f(R') - V_i(R')]$ at nuclear separation R'. As the nuclei move on the ground-state potential energy $V_i(R)$, the angular frequency $\Omega_{fi}(R)$ varies.

B. Semiclassical Time-Dependent Dipole Moment. Mukamel, Stern, and Warshel[7,8] discuss a variety of semiclassical approaches to electronic spectra, and what we illustrate here is perhaps the simplest and most classical of the possible choices. The semiclassical picture for the dipole moment which we use takes the nuclear motion to be classical and the electronic transition as a harmonic oscillator whose angular frequency Ω_{fi} is given by the energy difference between initial and final electronic state potential energy curves

$$\Omega_{fi} = \hbar^{-1}[V_f(\mathbf{r}^N) - V_i(\mathbf{r}^N)] \qquad (2.9)$$

in which $V_f(\mathbf{r}^N)$ is the final and $V_i(\mathbf{r}^N)$ is the initial electronic state potential energy as a function of the positions $\mathbf{r}^N \equiv \mathbf{r}_1, \ldots, \mathbf{r}_N$ of the N nuclei. Figure 1 illustrates this concept for a diatomic molecule.

We make the approximation that the frequency of the electronic oscillation is so much greater then that of the nuclear motions that we can evaluate the spectral density for clamped nuclei, i.e., for $\mathbf{r}^N$ fixed. Thus we may write $\mu(t)$, the electronic dipole moment at time t, as

$$\mu(t) = \mu_{fi}(\mathbf{r}^N)\exp[i\Omega_{fi}(\mathbf{r}^N)t] \qquad (2.10)$$

in which $\mu_{fi}(\mathbf{r}^N)$ gives the direction and magnitude of the electronic transition dipole moment between states i and f as a function of the positions $\mathbf{r}^N$ of the nuclei, i.e., the orientation and vibrational displacement of the molecule, and $\Omega_{fi}(\mathbf{r}^N)$ is the angular frequency of the electronic transition dipole oscillation at nuclear positions $\mathbf{r}^N$ derived by eq 2.9 from the difference in potential energies of the final and initial states at positions $\mathbf{r}^N$. The only time variation of $\mu(t)$ during the evaluation of the spectral density is that of $\exp(i\Omega_{fi}t)$.

This can be interpreted as the molecular equivalent to the semiclassical atomic "virtual harmonic oscillators" linked to atomic transitions which were used by Landenburg, Bohr, Kramers, Slater, Born, and others to describe the absorption, emission, and scattering of radiation by atoms, and which provided much of the groundwork for the eventual development of quantum mechanics.[9] The generalization to molecules is to make the frequency of the oscillator (corresponding to the electronic transition) vary with the positions of the nuclei following the energy difference between the potential curves of the final and initial states, clamping the nuclei in position while a spectral measurement is made, and then averaging over the distribution of nuclear positions $\mathbf{r}^N$ on the initial potential surface.

(4) R. G. Gordon, *Adv. Magn. Reson.*, **3**, 1 (1968).
(5) D. A. McQuarrie, "Statistical Mechanics", Harper and Row, New York, 1976.
(6) P. H. Berens and K. R. Wilson, *J. Chem. Phys.*, **74**, 4872 (1981).
(7) S. Mukamel, *J. Chem. Phys.*, **77**, 173 (1982).
(8) A. Warshel, P. S. Stern, and S. Mukamel, *J. Chem. Phys.*, 7498 (1983).
(9) B. L. van der Waerden, "Sources of Quantum Mechanics", North-Holland, Amsterdam, 1967.

Thus evaluating the spectral density[10] from eq 2.7b and 2.10

$$D[\hat{\epsilon}\cdot\mu] = |\hat{\epsilon}\cdot\mu_{fi}(\mathbf{r}^N)|^2\ \delta[\omega - \Omega_{fi}(\mathbf{r}^N)] \qquad (2.11)$$

in which $\delta[\omega - \Omega_{fi}(\mathbf{r}^N)]$ selects out the absorption frequency ω equal to $\Omega_{fi}(\mathbf{r}^N)$.

Then, the cross section $\sigma(\omega)$ for absorption frequency ω can be evaluated from eq 2.6, 2.8, and 2.11 as

$$\sigma(\omega) = \frac{4\pi^2\omega\gamma}{\hbar cn}\langle|\hat{\epsilon}\cdot\mu_{fi}(\mathbf{r}^N)|^2\ \eta[\omega - \Omega_{fi}(\mathbf{r}^N)]\rangle \qquad (2.12)$$

in which Ω_{fi} is given by eq 2.9, $\gamma = (1 - e^{-\beta\hbar\omega})$ for an equilibrium system and $\gamma = 1$ for a nonequilibrium system for which the density of final states ρ_f is essentially zero, and $\langle\rangle$ indicates an average over the positions $\mathbf{r}^N$ of the nuclei in the system. This average may be evaluated by molecular dynamics for arbitrary systems, and in addition by Monte Carlo or by explicit integration over the classical or quantum mechanical distribution of nuclear positions $\mathbf{r}^N$ for equilibrium systems.

We illustrate here the calculation of electronic spectra using molecular dynamics as we wish to make calculations of nonequilibrium transient spectra.[1,2] Thus, by computing the classical trajectories of the nuclei $\mathbf{r}^N(t)$ and knowing as a function of nuclear positions the electronic potential energies V_f and V_i as well as the electronic dipole moment μ_{fi} we can compute the electronic absorption spectrum in the manner shown. We take samples at different times during the trajectories of the nuclei and bin the instantaneous power spectra into appropriate intervals in frequency to accumulate the averaged spectrum.

If the system is an isotropic one, we can average eq 2.12 over all orientations to get[4-6]

$$\sigma(\omega) = \frac{4\pi^2\omega\gamma}{3\hbar cn}\langle|\mu_{fi}(\mathbf{r}^N)|^2\ \delta[\omega - \Omega_{fi}(\mathbf{r}^N)]\rangle \qquad (2.13)$$

C. Thermal Harmonic Quantum Correction. A simple quantum correction can be applied to the classical computation of equilibrium spectra to bring them into closer agreement with quantum reality. If we make the approximation that the nuclear motion of the system can be treated as harmonic oscillation, we find that the classical result can be quantum corrected by simply scaling the temperature at which the classical calculations are performed.

The exponential factor of the diagonal element of the density matrix for a harmonic oscillator at temperature T is[11]

$$\rho(x,x;T) \propto \exp\left[\frac{-m\omega}{\hbar}x^2 \tanh f\right] \qquad (2.14)$$

in which $f \equiv \hbar\omega/(2k_BT)$, k_B is Boltzmann's constant, x is the position, m is the mass, ω is the angular frequency of nuclear vibration, $\hbar$ is Planck's constant divided by 2π, and tanh is the hyperbolic tangent.

If we take the corresponding principle classical limit as $\hbar \to 0$ of eq 2.14, we find

$$\lim_{\hbar\to 0} \exp\left[\frac{-m\omega}{\hbar}x^2 \tanh f\right] = \exp\left[\frac{-m\omega^2x^2}{2k_BT}\right] = \exp\left[-\frac{V(x)}{k_BT}\right] \qquad (2.15)$$

in which, for a harmonic oscillator

$$V(x) = m\omega^2x^2/2 \qquad (2.16)$$

This correspondence principle result agrees with classical statistical mechanics. Now we compare the quantum and classical expressions, eq 2.14 and eq 2.15, to calculate the quantum correction. Let T be the physical temperature at which we wish to compute the spectra and let T' be the scaled temperature for a classical calculation, designed to replicate the quantum spectra at T.

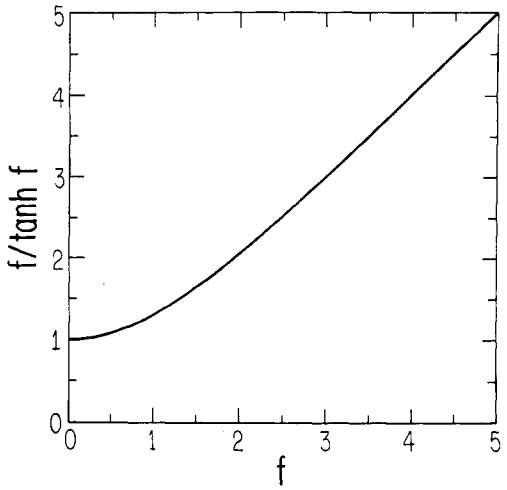

Figure 2. Graph of harmonic quantum correction factor $T'/T = f/\tanh f$, in which T is the true temperature and T' is the quantum corrected temperature at which the classical calculation is carried out and $f = \hbar\omega/(2k_BT)$.

$$\frac{-m\omega^2x^2}{2k_BT'} = \frac{-m\omega}{\hbar}x^2 \tanh f \qquad (2.17)$$

$$T' = \frac{\hbar\omega}{2k_B}\frac{1}{\tanh f} \qquad (2.18)$$

Dividing eq 2.18 by T gives the quantum correction factor C.

$$C = \frac{T'}{T} = \frac{\hbar\omega}{2k_BT}\frac{1}{\tanh f} = \frac{f}{\tanh f} \qquad (2.19)$$

This temperature quantum correction is plotted in Figure 2.

For example, the scaling factor used to compute the equilibrium electronic absorption spectrum for gas-phase I_2 at 298 K is $C = 1.03$. This means that if we perform the classical calculation at $T' = 307$ K then we will get the correct quantum spectral band contour in the approximation of harmonic motion as if we had done the quantum calculation at 298 K.

D. Symmetry. For a nonequilibrium system, the isotropic average of eq 2.13 will not in general be correct. Therefore we derive the proper averaging for the important case of pumping and probing with linearly polarized light. We determine the average of $D[\hat{\epsilon}\cdot\mu]$ over all orientations for the anisotropic and nonequilibrium case in which we prepare the sample by pumping it with linearly polarized light, and then measure its spectrum by probing with light polarized linearly in a different direction. For a diatomic molecule (symmetric top) the transition dipole μ_{fi} must either lie along the axis of the molecule or in a plane at right angles to the molecular axis. The absorption probability for pump light is dependent on the angle between the electric vector $\hat{\epsilon}'$ of the pump light and the transition dipole vector μ_{fi} and is greatest when μ_{fi} and $\hat{\epsilon}'$ are aligned,[12] and thus the pump light prepares an anisotropic sample of excited molecules, which can then be probed.

The angular distribution of excited molecules is[12]

$$I(\vartheta) = \frac{1}{4\pi}[1 + \beta P_2(\hat{\epsilon}'\cdot\hat{\mathbf{n}})] \qquad (2.20)$$

where the second-order Legendre polynomial is

$$P_2(x) = \frac{3x^2 - 1}{2} \qquad (2.21)$$

and ϑ is the angle between the electric unit vector $\hat{\epsilon}'$ of the pump light and the unit vector $\hat{\mathbf{n}}$ along the axis of I_2. The β term is

(10) F. G. Stremler, "Introduction to Communication Systems", Addison-Wesley, Reading, MA, 1977.

(11) R. P. Feynman, "Statistical Mechanics: A Set of Lectures", Benjamin/Cummings, Reading, MA 1979.

(12) R. N. Zare, *Mol. Photochem.*, **4**, 1 (1972).

referred to as the asymmetry parameter. When the transition dipole vector μ_{fi} points along the molecular axis, $\beta = 2$, a cosine-squared distribution. When μ_{fi} is perpendicular to the molecular axis, $\beta = -1$, a sine-squared distribution.

We would like to compute $\langle D[\hat{\epsilon}\cdot\mu]\rangle$ which determines the cross section for absorption by eq 2.6 and 2.8 in which $\langle\rangle$ indicates an average over all orientations for the distribution of the molecules which have been excited by the pump light. We can write this, using the notation of eq 2.7, as

$$\langle D[\hat{\epsilon}\cdot\mu]\rangle = \langle \sum_{ij} \hat{\epsilon}_i\hat{\epsilon}_j D[\mu_i,\mu_j]\rangle \tag{2.22a}$$

$$= \sum_{ij} \hat{\epsilon}_i\hat{\epsilon}_j \langle D[\mu_i,\mu_j]\rangle \tag{2.22b}$$

$$= \sum_{ij} \hat{\epsilon}_i\hat{\epsilon}_j A_{ij} \tag{2.22c}$$

in which the subscripts i and j refer to the Cartesian components of $\hat{\epsilon}$ and $\mu(t)$ and A_{ij} is the average of $D[\mu_i,\mu_j]$ over the orientational distribution of molecules excited by the pump light. We want

$$A_{ij} = \langle D[\mu_i,\mu_j]\rangle \tag{2.23a}$$

$$= \int d^2\hat{\mathbf{n}}\, I(\vartheta)\langle D[\mu_i,\mu_j]\rangle_{\hat{\mathbf{n}}} \tag{2.23b}$$

$$= \int \frac{d^2\hat{\mathbf{n}}}{4\pi}[1 + \beta P_2(\hat{\epsilon}'\cdot\hat{\mathbf{n}})]\langle D[\mu_i,\mu_j]\rangle_{\hat{\mathbf{n}}} \tag{2.23c}$$

in which $\hat{\mathbf{n}}$ is the unit vector along the axis of I_2 at the time of excitation, $I(\vartheta)$ is the probability distribution for excitation and $\langle D[\mu_i,\mu_j]\rangle_{\hat{\mathbf{n}}}$ is the average conditional on the axis of the molecules being fixed in a certain direction $\hat{\mathbf{n}}$ when the pump light is absorbed.

With rotational symmetry (see Appendix A)

$$\langle D[\mu_i,\mu_j]\rangle_{\hat{\mathbf{n}}} = A^{(0)}\delta_{ij} + A^{(2)}\frac{3\hat{n}_i\hat{n}_j - \delta_{ij}}{2} \tag{2.24}$$

so that for molecules with internuclear axes aligned along the z axis

$$\langle D[\mu_z,\mu_z]\rangle_{\hat{\mathbf{z}}} = A^{(0)} + A^{(2)} \tag{2.25}$$

$$\langle D[\mu_x,\mu_x]\rangle_{\hat{\mathbf{z}}} = \langle D[\mu_y,\mu_y]\rangle_{\hat{\mathbf{z}}} = A^{(0)} - \tfrac{1}{2}A^{(2)} \tag{2.26}$$

$$\tfrac{1}{3}\sum_{i=x,y,z}\langle D[\mu_i,\mu_j]\rangle_{\hat{\mathbf{z}}} = A^{(0)} \tag{2.27}$$

If we combine eq 2.24 with the following (see Appendix B)

$$\int \frac{d_2\hat{\mathbf{n}}}{4\pi}\,\hat{n}_i\hat{n}_j = \frac{1}{3}\delta_{ij} \tag{2.28}$$

$$\int \frac{d^2\hat{\mathbf{n}}}{4\pi}\,\hat{n}_i\hat{n}_j\hat{n}_k\hat{n}_l = \frac{1}{15}[\delta_{ij}\delta_{kl} + \delta_{ik}\delta_{jl} + \delta_{il}\delta_{jk}] \tag{2.29}$$

eq 2.23c can be evaluated as

$$A_{ij} = A^{(0)}\delta_{ij} + \beta A^{(2)}\frac{3\hat{\epsilon}'_i\hat{\epsilon}'_j - \delta_{ij}}{10} \tag{2.30}$$

Finally, we write our average from eq 2.23c as

$$\langle D[\hat{\epsilon}\cdot\mu]\rangle = \sum_{ij}\hat{\epsilon}_i\hat{\epsilon}_j\left[A^{(0)}\,\delta_{ij} + \beta A^{(2)}\frac{3\hat{\epsilon}'_i\hat{\epsilon}'_j - \delta_{ij}}{10}\right] \tag{2.31a}$$

$$= A^{(0)} + \beta A^{(2)}\frac{3(\hat{\epsilon}'\cdot\hat{\epsilon})^2 - 1}{10} \tag{2.31b}$$

$$= A^{(0)} + \frac{\beta}{5}A^{(2)}P_2(\hat{\epsilon}'\cdot\hat{\epsilon}) \tag{2.31c}$$

in which $\hat{\epsilon}'$ is the electric unit vector of the pump light and $\hat{\epsilon}$ is the electric unit vector of the probe light.

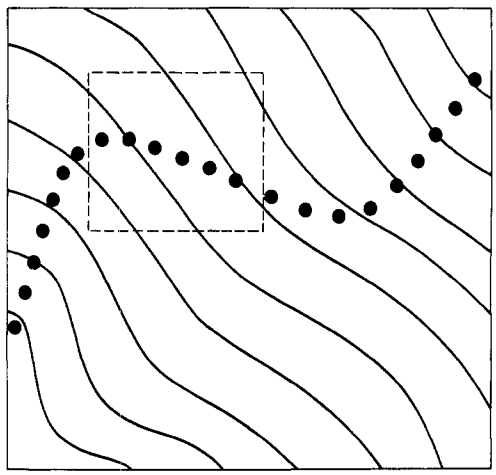

Figure 3. A two-dimensional contour plot of $V_f(\mathbf{r}^N) - V_i(\mathbf{r}^N)$ showing a particular trajectory on the V_i potential surface plotted as solid circles spaced at equal times. The inset box (dashed lines) is magnified in Figure 4.

Therefore, to compute the absorption spectrum for probe light polarized along $\hat{\epsilon}$ by a system prepared by pump light polarized along $\hat{\epsilon}'$

$$\sigma(\omega) = \frac{4\pi^2\omega\gamma}{\hbar cn}\left[A^{(0)} + \frac{\beta}{5}A^{(2)}P_2(\hat{\epsilon}'\cdot\hat{\epsilon})\right] \tag{2.32}$$

in which

$$A^{(0)} = \tfrac{1}{3}\langle|\mu_{fi}(\mathbf{r}^N)|^2\,\delta[\omega - \Omega_{fi}(\mathbf{r}^N)]\rangle \tag{2.33}$$

$$A^{(2)} = \langle[\hat{\mathbf{n}}\cdot\mu_{fi}(\mathbf{r}^N)]^2\,\delta[\omega - \Omega_{fi}(\mathbf{r}^N)]\rangle_{\hat{\mathbf{n}}} - A^{(0)} \tag{2.34}$$

where β is the asymmetry parameter defined above for the pump light, $\mu_{fi}(\mathbf{r}^N)$ is the transition dipole vector at nuclear positions $\mathbf{r}^N$ for the probe light, and $\langle[\hat{\mathbf{n}}\cdot\mu_{fi}(\mathbf{r}^N)]^2\rangle_{\hat{\mathbf{n}}}$ is the average of the $\hat{\mathbf{n}}$ component squared of the probe transition moment vector at nuclear positions $\mathbf{r}^N$ for molecules with symmetry axis aligned along $\hat{\mathbf{n}}$ when the pump light is absorbed.

III. Relation to Other Techniques

The almost classical technique we illustrate here is related to other semiclassical techniques for computing electronic absorption spectra.[7,8] This approach is related to a short time limit of the wave packet time-dependent method.[3,13-16] Thus, it is appropriate for liquid solutions with rapid randomization (which can also be treated by wavepacket techniques[17]), for excitation to quickly dissociating states, and for the band contours of systems with vibrational and rotational structure, the details of which would be given by longer time wave packet evolution.

In this section we show the equivalence of the binning method used for calculations in this paper and the semiclassical methods of Lax,[18] and Tellinghuisen and Moeller,[19] and Lee,[20] Lax's discussion[18] of the relation of "exact" and classical Franck-Condon spectra applies equally to the comparison of "exact" wavepacket and molecular dynamic binning spectra, and his semiclassical Franck-Condon spectra are approximated by our harmonic quantum correction. The Landau-Zener-Stuckelberg surface crossing probability, in a form similar to the Tully-Preston surface hopping method,[21] is shown to give the same results as the other methods when the lower surface is raised by $\hbar\omega$, giving rise to

(13) S.-Y. Lee and E. J. Heller, *J. Chem. Phys.*, **76**, 3035 (1982).
(14) E. J. Heller, *J. Chem. Phys.*, **68**, 2066 (1978).
(15) E. J. Heller, *Acc. Chem. Res.*, **14**, 368 (1981).
(16) E. J. Heller in "Potential Energy Surfaces and Dynamics Calculations", D. Truhlar, Ed., Plenum Press, New York, 1981.
(17) E. J. Heller, J. R. Reimers, and K. R. Wilson, *J. Chem. Phys.*, to be submitted.
(18) M. Lax, *J. Chem. Phys.*, **20**, 1752 (1952).
(19) J. Tellinghuisen and M. B. Moeller, *Chem. Phys.*, **50**, 301 (1980).
(20) S.-Y. Lee, *J. Chem. Phys.*, **76**, 3064 (1982).
(21) J. C. Tully in "Dynamics of Molecular Collisions", Vol. 2, W. H. Miller, Ed., Plenum, New York, 1976, p 217.

intersection(s) of the ground- and excited-state surfaces, which can be treated as surface crossings with a strength given by the usual dipole coupling. The binning method given in this paper is considerably simpler, both conceptually and computationally, than the other methods mentioned above, so it is important to establish the equivalence. In addition, the extension of the molecular dynamic binning method to nonequilibrium systems[1,2] is particularly clear and simple.

A. The Molecular Dynamic Binning Method. Consider Figure 3 which shows, for a two-dimensional case, a contour plot of $V_f(\mathbf{r}^N) - V_i(\mathbf{r}^N)$, together with a particular trajectory on the V_i potential surface. This trajectory is plotted as dots spaced at equal times, which are the sample times used to inquire as to which bin the trajectory is in. The space between a pair of contour lines corresponds to a frequency range

$$\omega_k - \frac{\delta\omega}{2} \leq \omega \leq \omega_k + \frac{\delta\omega}{2} \tag{3.1}$$

where $\omega_k = k\,\delta\omega$, i.e., the kth bin. (The contour intervals are then $\delta E = \hbar\,\delta\omega$.) In Figure 4 we magnify a portion of Figure 3 and show a few more details. The amount of time spent between the two contour lines shown is proportional to the contribution this particular trajectory segment will make to the corresponding spectral frequency bin. The time τ spent between contours is the distance D traversed divided by the velocity, or

$$\tau = \frac{D}{(p/m)} = \frac{md}{p\sin\vartheta} = \frac{md}{p_\perp} \tag{3.2}$$

in which p is the magnitude of the momentum, $p_\perp = p\sin\vartheta$ is the magnitude of the momentum perpendicular to the contour lines, and m the mass. The perpendicular separation d between the contours is

$$d = \frac{\hbar\,\delta\omega}{|\Delta F_\perp|} \tag{3.3}$$

where

$$|\Delta F_\perp| = |\nabla[V_f(\mathbf{r}^N) - V_i(\mathbf{r}^N)]| \tag{3.4}$$

evaluated in the vicinity of the crossing region. $\Delta F_\perp$ is the force change between the final and initial potential surfaces perpendicular to the contour lines of $V_f - V_i$ at the intersection $V_i + \hbar\omega_m = V_f$. If we take the rate of crossing per unit time from the initial to the final surface to be

$$k = \frac{2\pi W^2}{\hbar^2\,\delta\omega} \tag{3.5}$$

in which W is a coupling parameter, the total probability P of crossing from the initial to the final surface while on the trajectory in the region of the bin is

$$P = k\tau = \frac{2\pi W^2}{\hbar^2\,\delta\omega}\frac{1}{p_\perp}\left[\frac{m\hbar\,\delta\omega}{|\Delta F_\perp|}\right] \tag{3.6a}$$

$$= \frac{2\pi W^2}{\hbar}\left[\frac{m}{p_\perp|\Delta F_\perp|}\right] \tag{3.6b}$$

Nothing essential depends on our assumption of two degrees of freedom, and eq 3.6 is general.

B. Equivalence with the Landau–Zener–Stuckelberg, Tully–Preston (LZSTP) Method. Equation 3.6 is just the Landau–Zener–Stuckelberg rate for radiationless transition surface crossing[21,22] in the case of diabatic surfaces which intersect with small coupling W. (The adiabatic crossing probability would be $1 - P$.) The multidimensional picture of a hopping trajectory is due to Tully and Preston.[21] The calculation of the rate of crossing, as opposed to following the trajectories after they have crossed (which we do not need to do), has been recently carried out in the context of radiationless transitions ($\omega = 0$) by Heller and Brown[22] (who did not use the simplified binning method), and the results are excellent.

For coupling W caused by dipole radiation, we have, for unit field strength

$$W^2(\mathbf{r}^N) = \frac{1}{n}|\mu_{fi}(\mathbf{r}^N)|^2 \tag{3.7}$$

in which n is the index of refraction.

C. Equivalence with the "Classical" Method. It is possible to arrive in several different ways at a semiclassical expression for the absorption cross section which involves only classical (possibly quantum corrected) phase space densities. Lax[18] was apparently the first to derive it. Lee[20] calls it the "semiclassical" cross section, and Tellinghuisen and Moeller[19] call it, as we do here, the classical absorption spectrum. Indeed, we arrived at their formula in section II in yet another way, i.e., the classical oscillating dipole analogy of the old quantum theory.

To show the equivalence of eq 2.13 and eq 25 of Tellinghuisen and Moeller[19] to the binning method and LZSTP, we need to relate the individual trajectory picture used in sections IIIA and IIIB to the coordinate space integral expression, eq 2.13.

The concept of the binning method is easiest to work with. We imagine pointwise sampling the appropriate phase space density $\rho(\mathbf{r}^N,\mathbf{p}^N)$, which may be equilibrium or nonequilibrium. We merely check to see what bins the phase space points are in, and assign them appropriately, thus building a histogram of the absorption profile. There is no need to run the trajectories, other than as a means to compute $\rho(\mathbf{r}^N,\mathbf{p}^N)$, since in the short time required to cross a bin the overall phase space density is not changing much (or for a stationary $\rho(\mathbf{r}^N,\mathbf{p}^N)$ not changing at all). Also, momentum is irrelevant as to which frequency bin the phase space point belongs. Thus, the total rate of crossing induced by the electromagnetic field is the bin count over all of phase space, or

$$k = \frac{2\pi}{3\hbar\,\delta\omega}\int d\mathbf{r}^N\,d\mathbf{p}^N\,\rho(\mathbf{r}^N,\mathbf{p}^N)W^2(\mathbf{r}^N)\,\Delta(\omega - \Omega_{fi}) \tag{3.8a}$$

$$= \frac{2\pi}{3\hbar n\,\delta\omega}\int d\mathbf{r}^N\,P(\mathbf{r}^N)|\mu_{fi}(\mathbf{r}^N)|^2\,\Delta(\omega - \Omega_{fi}) \tag{3.8b}$$

where $P(\mathbf{r}^N)$ is the probability as a function of position, the factor of $^1/_3$ is introduced for spherically averaged molecular orientations, and

$$\Delta(X) = 1 \quad -\delta\omega/2 \leq X \leq \delta\omega/2$$
$$= 0 \quad \text{otherwise}$$

Now take the limit as $\delta\omega \to 0$

$$k = \frac{2\pi}{3\hbar n}\int d\mathbf{r}^N\,P(\mathbf{r}^N)|\mu_{fi}(\mathbf{r}^N)|^2\,\sigma(\omega - \Omega_{fi}) \tag{3.8c}$$

To relate this rate to a cross section, we note that for unit field strength the photon flux is $c/(2\pi\omega)$, and $\sigma \times$ flux = rate, thus

$$\sigma(\omega) = \frac{4\pi^2\omega}{3\hbar cn}\int d\mathbf{r}^N\,P(\mathbf{r}^N)|\mu_{fi}(\mathbf{r}^N)|^2\,\sigma(\omega - \Omega_{fi}) \tag{3.8d}$$

$$= \frac{4\pi^2\omega}{3\hbar cn}\langle|\mu_{fi}(\mathbf{r}^N)|^2\,\delta[\omega - \Omega_{fi}(\mathbf{r}^N)]\rangle \tag{3.8e}$$

Equation 3.8d is the multidimensional form of the diatomic work of Tellinghuisen and Moeller[19] (see also Lax[18] and Lee[20]), and eq 3.8e is eq 2.13 of this paper. As this equation is derived from the binning method, the equivalence is thus established between LZSTP, the binning method, and the "classical spectrum".

D. Relation to the Reflection Method. It is natural to seek the relation to the reflection approximation, probably the most used technique for estimation of absorption spectra in diatomic molecules. Heller[14] and Lee, Brown, and Heller[23] have given the correct polyatomic generalization of the reflection method. It is related but not equivalent to the methods of sections IIIA–C. For low-lying vibrational levels of V_i and steep upper surfaces the

(22) E. J. Heller and R. C. Brown, *J. Chem. Phys.*, in press.

(23) S.-Y. Lee, R. C. Brown, and E. J. Heller, *J. Phys. Chem.*, 87, 2045 (1983).

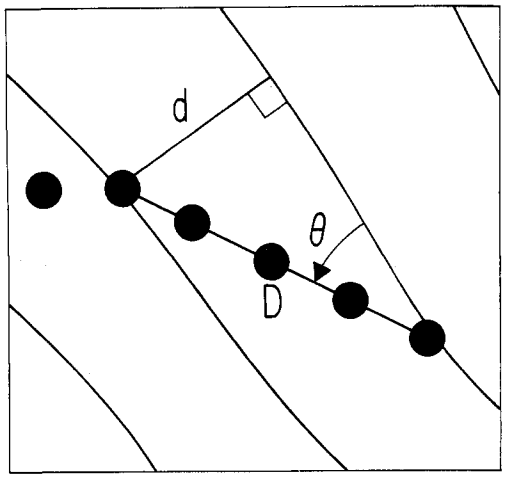

Figure 4. A magnified view of the inset box of Figure 3. D is the distance traversed between adjacent contour lines and d is the perpendicular distance between the contour lines.

reflection method should be superior to classical absorption techniques.

As Tellinghuisen and Moeller[19] have noted, the reflection approximation has its drawbacks, especially for moderate and high temperatures, since each quantum wave function with significant Boltzmann populations must be known and used. The higher vibrational states give rise to inaccurate results (for a discussion of this see Heller[14]), and the method is therefore suspect at high temperatures, where it is also most difficult to apply. Here, the classical spectrum methods are distinctly advantageous.

The reflection approximation, in the present notation, is

$$\sigma(\omega) = \frac{4\pi^2\omega}{3\hbar cn}\sum_j \int d\mathbf{r}^N\, |\Psi_{ij}(\mathbf{r}^N)|^2 |\mu_{fi}(\mathbf{r}^N)|^2\, \delta\{\omega - [V_f(\mathbf{r}^N) - E_{ij}]\} \tag{3.9}$$

The main distinction between eq 3.9 and eq 3.8 is the replacement of $V_i(\mathbf{r}^N)$ by E_{ij}, the energy of the jth vibronic state on the initial surface i, and the enumeration of each initial wave function $\Psi_{ij}(\mathbf{r}^N)$.

E. Wavepacket Methods. Wavepacket dynamics can also be used to compute electronic spectra[3,17] and provides a route to more exact solutions. In a semiclassical version the method is efficient but not as fast as the more classical methods (especially the binning method) discussed here. However, use of the coherent wavepacket approach permits accurate rendition of the spectrum, including interference oscillations and spectral structure not available in any of the methods mentioned above. There are no restrictions to low or high temperatures, but for highly anharmonic potentials approximate wavepacket propagation methods[3] can have significant errors for higher resolution spectra and more exact propagation may be required.[13]

IV. Inputs to I_2 Calculation

In this section, we test the binning molecular dynamics method, computing the band contour of the visible absorption spectrum of room temperature gas-phase I_2 molecules, and compare the results to experimental measurements.

A. Potential Energy. Figure 5 shows the potential energy curves for the iodine ground X $0_g^+(^1\Sigma)$ state and the excited A $1_u(^3\Pi)$, B $0_u^+(^3\Pi)$, and B″ $1_u(^1\Pi)$ states. The ground X state is taken from a semiempirical potential due to Matzen, Calder, and Hoffman[24] and from the experimental RKR values of Coxon.[25] The A state and the B″ repulsive state are from Tellinghuisen,[26,27] and the B state is from Barrow and Yee[28] and Luc.[29]

For the ground state for internuclear distance $R < 0.325$ nm and for the entire B″ state the potential energies are easily calculated from potential functions $V(R)$ cited above. The ground state for $R \geq 0.325$ nm, the A state, and the B state potential energy values are generated by the Aitken–Neville technique[30] of iterated linear interpolation of the RKR turning points, a set of n points $V(R_i)$, i = 0, ..., n where $V(R_i)$ is the potential energy at internuclear distance R_i. Interpolation methods use function points to determine a unique polynomial $P_n(R)$ which satisfies the constraints

$$P_n(R_i) = V(R_i) \qquad i = 0, ..., n \tag{4.1}$$

The Aitken–Neville method uses repeated linear interpolation to compute the value of $P_n(X)$ for X in (R_o,R_n) subject to the constraints that $P_n(R_i) = V(R_i)$. Here X is an internuclear distance for which a value of the potential energy $V(X)$ is required. Ten function points $V(R_i)$, i = m − 9, ..., m, are used in the interpolation to compute $P_m(X) \equiv V(X)$. These points are a subset of the complete set of RKR points. The range (R_{m-9},R_m) is chosen such that X lies as close as possible to the median value. In the case where X is close to R_o or R_n, where n is the total number of RKR points, there are still ten points used in the interpolation.

The upper portions of the inner repulsive branch of the A state and the B state are approximated by potentials of the form $V(R) = A + C/R^n$. In the case of the B state repulsive branch $C = 8.2805 \times 10^{-6}$, n = 12 and $A = 164.60$. The smooth curve is attached at $v' = 34$. For the A state repulsive branch $C = 3.538 \times 10^{-5}$, n = 11, $A = 104.87$, and the curve is attached at $v' = 35$. Here the units of A and C are such that $V(R)$ is in kJ mol^{-1} when R is in nanometers.

B. Transition Dipole. The transitions strengths $|\mu_{fi}|^2$ for the A ← X transition and the B″ ← X transition are taken to be constant as a function of internuclear distance, with values[27] $|\mu_{fi}|_{A\leftarrow X}^2 = 0.453 \times 10^{-60}$ C^2 m^2 (0.0407 D^2) and $|\mu_{fi}|_{B''\leftarrow X}^2 = 1.5135 \times 10^{-60}$ C^2 m^2 (0.136 D^2), in which D is Debyes (e Å). For the B ← X transition the electronic transition moment $|\mu_{fi}|_{B\leftarrow X}$ vs. R centroid is derived over the range $R = 0.25$ to $R = 0.29$ nm from the transition dipole data.[27] The data points for $|\mu_{fi}|$ from Tellinghuisen[27] are used to construct two linear segments for the intervals $R = 0.25$ to 0.2685 nm and $R = 0.2685$ to 0.29 nm. The resulting $|\mu_{fi}|$ vs. internuclear distance functions for the three transitions are shown in Figure 6.

V. Computational Method

To compute the classical trajectories[31] $\mathbf{r}^N(t) = \mathbf{r}_1(t), ..., \mathbf{r}_N(t)$ we first choose an initial set of coordinates and momenta for the N atoms in our system and then describe the atomic motion by integrating Newton's second law

$$-\frac{\delta V}{\delta \mathbf{r}_i} = \mathbf{F}_i = m_i\frac{d^2\mathbf{r}_i}{dt^2} \qquad i = 1, ..., N \tag{3.2}$$

in which $V = \delta V(\mathbf{r}^N)$ is the potential energy of the atoms at positions $\mathbf{r}_1, ..., \mathbf{r}_N$, $\mathbf{F}_i = \mathbf{F}_i(\mathbf{r}^N)$ is the force on the ith atom, and m_i is the mass of the ith atom. The time step size is 1.0 fs. A modified Verlet integration algorithm is used[32-34] along with minimum image periodic truncated octahedral boundary conditions[35] to reduce edge effects.

Before we actually make spectral calculations, we equilibrate the system at the desired temperature T by integrating forward in time, stopping at intervals to choose a new set of velocities selected at random from a Maxwell–Boltzmann distribution consistent with the temperature T. Then, to sample more of configuration space, we again pick new sets of velocities between

(24) M. K. Matzen, G. V. Calder, and D. K. Hoffman, *Spectrochim. Acta, Part A*, **29**, 2005 (1973).
(25) J. A. Coxon, *J. Quant. Spectrosc. Radiat. Transfer*, **11**, 443 (1971).
(26) J. Tellinghuisen, *J. Mol. Spectrosc.*, **86**, 393 (1981).
(27) J. Tellinghuisen, *J. Chem. Phys.*, **76**, 4736 (1982).
(28) R. F. Barrow and K. K. Yee, *J. Chem. Soc., Faraday Trans. 2*, **69**, 684 (1973).
(29) P. Luc, *J. Mol. Spectrosc.*, **80**, 41 (1980).
(30) T. R. McCalla, "Introduction to Numerical Methods and FORTRAN Programming", Wiley, New York, 1967.
(31) P. H. Berens and K. R. Wilson, *J. Comp. Chem.*, **4**, 313 (1983).
(32) D. Beeman, *J. Comput. Phys.*, **20**, 130 (1976).
(33) H. C. Andersen, Stanford, private communication.
(34) R. W. Hockney and J. W. Eastwood, "Computer Simulation Using Particles", McGraw-Hill, New York, 1981.
(35) D. J. Adams in "The Problem of Long-Range Forces in the Computer Simulation of Condensed Media", D. Ceperely, Ed., National Resource for Computation in Chemistry, Berkeley, 1980, p 13.

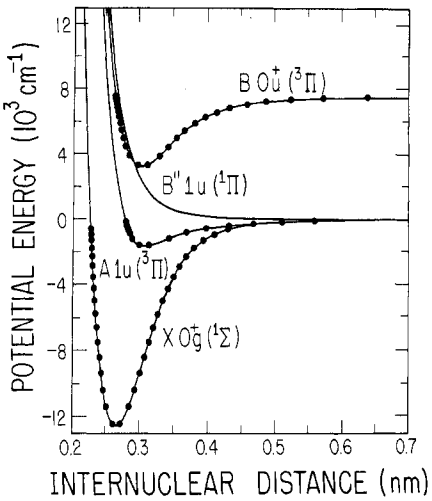

Figure 5. The potential energy curves for the ground X $0_g^+(^1\Sigma)$, A $1_u(^3\Pi)$, B $0_u^+(^3\Pi)$, and B'' $1_u(^1\Pi)$ states used in the calculation of the electronic absorption spectrum of iodine. The dots show the RKR turning points for every fifth vibrational level.

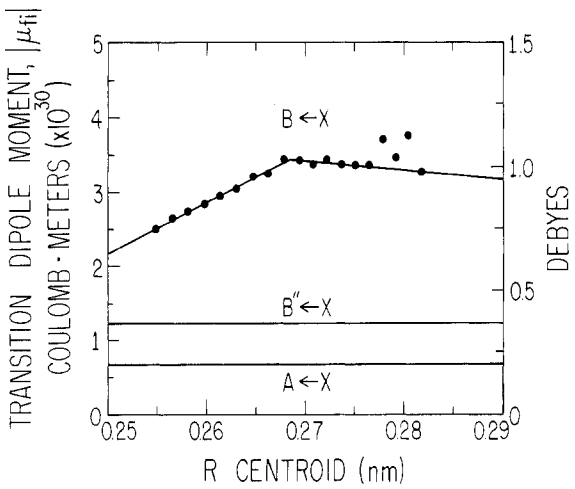

Figure 6. Transition dipole moment magnitudes $|\mu_{fi}(R)|$ as functions of I_2 internuclear distance R. For the A ← X and the B'' ← X transitions the function is taken to be a constant while for the B ← X transition it is shown as a function of R centroid. The solid circles are the data points from Tellinghuisen.

sets of trajectories used for the spectral calculations, and average the resulting spectra.

The classical trajectories for a system of 100 noninteracting I_2 molecules were computed for a time period of 6 ns.

VI. I_2 Equilibrium Gas-Phase Spectrum

Figure 7 shows the equilibrium gas-phase spectrum of I_2 as calculated by molecular dynamics and the gas-phase experimental data from Tellinghuisen[27] superimposed as solid circles. The solid line is the quantum corrected gas-phase spectrum while the dashed line is the uncorrected gas-phase spectrum. There is very good agreement between the theoretical and experimental electronic absorption band contours of I_2 and the quantum correction is seen to be small for this case of low ground-state vibrational frequency.

VII. Discussion and Conclusion

We have shown that the band contour of the electronic absorption spectrum of a gas-phase equilibrium system can be computed by a nearly classical mechanical approach and have used I_2 as an illustration. Utilizing potential energy and transition moment functions from the literature, we have been able to calculate the electronic absorption spectral band contour to a remarkable accuracy. Furthermore we have shown that a quantum correction can be applied to the classically computed spectrum, but that for the massive, weakly bound I_2 molecule this

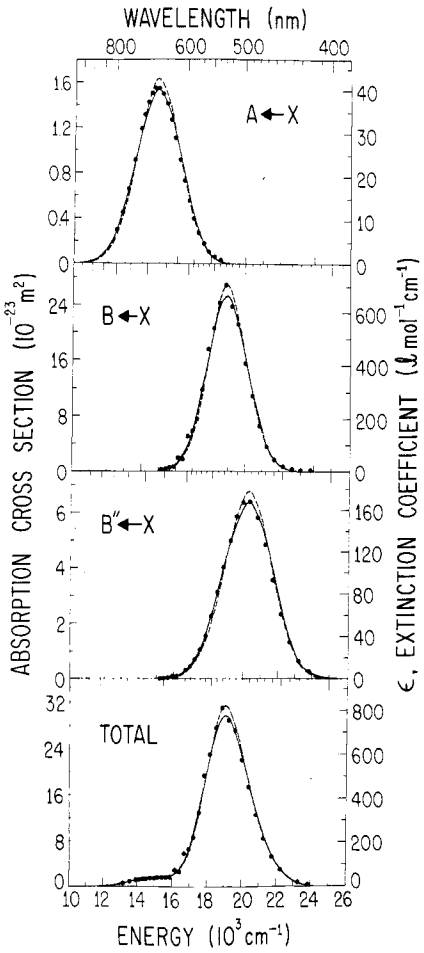

Figure 7. Comparison of I_2 equilibrium electronic absorption band contours at 298 K as calculated by molecular dynamics with the gas-phase experimental values (solid circles) as given by Tellinghuisen. The nonquantum corrected spectra are shown as dashed lines and the quantum corrected as solid lines. The figure shows the separate contributions of the A $1_u(^3\Pi)$, B $0_u^+(^3\Pi)$, and B'' $1_u(^1\Pi)$ excited states and the total absorption spectrum, in which ϵ is the decadic molar extinction coefficient.

correction is quite small. Since classical molecular dynamics are the basis of these calculations one can have confidence, given the agreement of computed and measured spectral contours, that the classical nuclear motions as simulated are a reasonable classical representation of the actual nuclear time evolution of the real system.

Another very different way to compute such spectra ab initio from molecular dynamics would be to use a quantum force classical trajectory (QFCT) method[36] in which we follow a classical trajectory, computing at each time step the electronic transition dipole vector $\mu_{fi}(\mathbf{r}^N)$ and the potential energies $V_f(\mathbf{r}^N)$ and $V_i(\mathbf{r}^N)$ of the final and initial states in order to calculate the transition dipole frequency $\Omega_{fi}(\mathbf{r}^N)$, and to bin the results to accumulate the spectrum.

Calculations of electronic band contours with the method presented here are particularly appropriate for the liquid state in which the rotational and much of the vibrational structure is washed out by dephasing due to averaging over solvent molecule initial conditions and by different interactions with solvent molecules in the ground and excited states.[17] We have illustrated liquid-state calculations elsewhere[1,2] using the technique presented in this paper. Due to the simplicity and close connection to classical trajectories, we can also easily carry out nonequilibrium time-dependent calculations as we have already shown[1,2] to compute the transient absorption during chemical reactions in solution.

(36) D R. Fredkin, A. Komornicki, S. R. White, and K. R. Wilson, *J. Chem. Phys.*, **78**, 7077 (1983).

11	22	33	23	32	31	13	12	21
1 0	0	0	$1/2^{1/2}$	$1/2^{1/2}$	0	0	0	0
2 0	0	0	0	0	$1/2^{1/2}$	$1/2^{1/2}$	0	0
3 0	0	0	0	0	0	0	$1/2^{1/2}$	$1/2^{1/2}$
4 $1/6^{1/2}$	$1/6^{1/2}$	$-2/6^{1/2}$	0	0	0	0	0	0
5 $1/2^{1/2}$	$-1/2^{1/2}$	0	0	0	0	0	0	0

(B2)

Acknowledgment. We thank the National Aeronautics and Space Administration, Ames Research Center, the Department of Energy, the National Science Foundation, Chemistry, the Office of Naval Research, Chemistry, and the National Institute of Health, Division of Research Resources for providing the support which made this work possible.

Appendix A. Proof of Eq 2.24

We wish to explore the consequences of rotational symmetry for the structure of the quantity

$$A_{ij}(\hat{\mathbf{n}}) = \langle D[\mu_i,\mu_j]\rangle_{\hat{\mathbf{n}}} \tag{A1}$$

For any (proper or improper) rotation $R = [R_{ij}]$, rotational invariance implies that

$$A_{ij}(R\hat{\mathbf{n}}) = \sum_{kl} R_{ik}R_{jl}A_{kl}(\hat{\mathbf{n}}) \tag{A2}$$

as can be seen by recognizing that, for any pair of vectors **a** and **b**, $\sum A_{ij}(\hat{\mathbf{n}})a_ib_j$ is invariant under rigid rotation of the triple **a**, **b**, $\hat{\mathbf{n}}$.

First consider the case $\hat{\mathbf{n}} = \hat{\mathbf{z}}$ and R a rotation by φ about the **z** axis. Differentiating eq A2 with respect to φ and then setting φ to zero yields

$$\begin{bmatrix} A_{12}(\hat{z}) + A_{21}(\hat{z}) & A_{22}(\hat{z}) - A_{11}(\hat{z}) & A_{23}(\hat{z}) \\ A_{22}(\hat{z}) - A_{11}(\hat{z}) & -A_{12}(\hat{z}) - A_{21}(\hat{z}) & -A_{13}(\hat{z}) \\ A_{32}(\hat{z}) & -A_{31}(z) & 0 \end{bmatrix} = 0 \tag{A3}$$

from which we conclude that

$$A(\hat{z}) = \begin{bmatrix} A^{(0)} - {}^1/_2A^{(2)} & -A^{(1)} & 0 \\ A^{(1)} & A^{(0)} - {}^1/_2A^{(2)} & 0 \\ 0 & 0 & A^{(0)} + A^{(2)} \end{bmatrix} \tag{A4}$$

for appropriate constants $A^{(i)}$, $i = 1, 2, 3$.

Next, invoke eq A2 for $\hat{\mathbf{n}} = \hat{\mathbf{z}}$ and R the improper rotation (reflection in the xz plane). We are *not* assuming that the excitable molecule has an inversion center, any more than we assumed the excitable molecule to be spherically symmetric in the preceding paragraph.

$$R = \begin{bmatrix} 1 & 0 & 0 \\ 0 & -1 & 0 \\ 0 & 0 & 1 \end{bmatrix} \tag{A5}$$

Using eq A5 and A3 in A2 yields $A^{(1)} = -A^{(1)}$, so $A^{(1)} = 0$.

We can write eq A3, with $A^{(1)} = 0$, in the form

$$A_{ij}(\hat{\mathbf{z}}) = A^{(0)}\delta_{ij} + A^{(2)}\frac{3\delta_{i3}\delta_{i3} - \delta_{ij}}{2} \tag{A6}$$

Now choose any rotation R such that $R\hat{\mathbf{z}} = \hat{\mathbf{n}}$, i.e., $R_{i3} = \hat{n}_i$, $i = 1, 2, 3$. Using eq A2 and A6, we have

$$A_{ij}(\hat{\mathbf{n}}) = A_{ij}(R\hat{\mathbf{z}}) = \sum_{kl} R_{ik}R_{jl}A_{kl}(\hat{\mathbf{z}}) = \sum_{kl} R_{ik}R_{jl}\left[A^{(0)}\delta_{kl} + A^{(2)}\frac{3\delta_{k3}\delta_{l3} - \delta_{kl}}{2}\right] = A^{(0)}\delta_{ij} + A^{(2)}\frac{3\hat{n}_i\hat{n}_j - \delta_{ij}}{2} \tag{A7}$$

where, in the last step we used the orthogonality of R

$$\sum R_{ik}R_{jl}\delta_{kl} = \sum R_{ik}R_{jk} = \delta_{ij} \tag{A8}$$

and $R\hat{\mathbf{z}} = \hat{\mathbf{n}}$ (so that $\sum R_{ik}\delta_{k3} = R_{i3} = \hat{n}_i$). With the definition eq A1, eq A7 is identical with eq 2.24, which we set out to prove.

Appendix B. Proof of Eqs 2.28 and 2.29

Define the linear map

$$M\colon E^3 \otimes E^3 \to E^5 \tag{B1}$$

where E^n is the real linear space of n-tuples, by the matrix (B2), M is the matrix that couples two p states to a d state. From (B2) it is easy to read off that $MM^T = 1$ (the identity matrix on E^5) and that $P = M^TM$ is the projection (on d states) whose matrix is

$$P_{ij,kl} = {}^1/_2[\delta_{ik}\delta_{jl} + \delta_{il}\delta_{jk} - {}^2/_3\delta_{ij}\delta_{kl}] \tag{B3}$$

The point of introducing M is that, for any rotation R, there is a 5×5 matrix $\Gamma(R)$ such that

$$MR \otimes R = \Gamma(R)M \tag{B4}$$

and $\Gamma(R)$ is a unitary irreducible representation of the rotation group.

1. The existence of $\Gamma(R)$ and its being an irreducible representation follow from the observation that the polynomials

$$\sum_{ij} M_{\mu,ij}x_ix_j \tag{B5}$$

are d state wave functions.

2. The unitarily of $\Gamma(R)$ follows from

$$\Gamma(R)\Gamma(R)^T = MR \otimes RM^TMR^{-1} \otimes R^{-1}M^T = MR \otimes RPR^{-1} \otimes R^{-1}M^T = MPM^T = MM^TMM^T = 1 \tag{B6}$$

thanks to the consequence

$$R \otimes RPR^{-1} \otimes R^{-1} = P \tag{B7}$$

of the orthogonality of R.

We are now prepared to evaluate rotational averages (2.28) and (2.29). Using (B3)

$$M^TM\hat{\mathbf{n}} \otimes \hat{\mathbf{n}} = P\,\hat{\mathbf{n}} \otimes \hat{\mathbf{n}} = \hat{\mathbf{n}} \otimes \hat{\mathbf{n}} - {}^1/_3\delta \tag{B8}$$

so, with the definition

$$v(\hat{\mathbf{n}}) = M\hat{\mathbf{n}} \otimes \hat{\mathbf{n}} \tag{B9}$$

and the observation, which follows from (B4) and (B9)

$$v(R\hat{\mathbf{n}}) = MR \otimes R\hat{\mathbf{n}} \otimes \hat{\mathbf{n}} = \Gamma(R)M\hat{\mathbf{n}} \otimes \hat{\mathbf{n}} = \Gamma(R)v(\hat{\mathbf{n}}) \tag{B10}$$

we have a decomposition of $\hat{\mathbf{n}} \otimes \hat{\mathbf{n}}$

$$\hat{\mathbf{n}} \otimes \hat{\mathbf{n}} = {}^1/_3\delta + M^Tv(\hat{\mathbf{n}}) \tag{B11}$$

into components transforming by the one- and five-dimensional irreducible representations of the rotation group. The strategy for evaluating averages $\langle f(\hat{\mathbf{n}})\rangle$ over the unit sphere is to replace them with averages over the rotation group $\langle f(R\hat{\mathbf{z}})\rangle$, and use the orthogonality theorem of group representation theory.[37] In this way, we find

$$\langle v(\hat{\mathbf{n}})\rangle = \langle \Gamma(R)\rangle v(\hat{\mathbf{z}}) = 0 \tag{B12}$$

which, with (B11), proves (2.28), and

$$\langle v_\alpha(\hat{\mathbf{n}})v_\beta(\hat{\mathbf{n}})\rangle = \sum_{\mu\nu}\langle \Gamma_{\alpha\mu}(R)\Gamma_{\beta\nu}(R)\rangle v_\mu(\hat{\mathbf{z}})v_\nu(\hat{\mathbf{z}}) = \sum_{\mu\nu}(1/5)\delta_{\alpha\beta}\delta_{\mu\nu}v_\mu(\hat{\mathbf{z}})v_\nu(\hat{\mathbf{z}}) = (1/5)\delta_{\alpha\beta}P_{33,33} = (2/15)\delta_{\alpha\beta} \tag{B13}$$

which, with (B11), yields

$$\langle \hat{\mathbf{n}}_i\hat{\mathbf{n}}_j\hat{\mathbf{n}}_k\hat{\mathbf{n}}_l\rangle = (1/9)\delta_{ij}\delta_{kl} + \sum_{\alpha\beta} M_{\alpha,ij}M_{\beta,kl}\langle v_\alpha(\hat{\mathbf{n}})v_\beta(\hat{\mathbf{n}})\rangle = (1/9)\delta_{ij}\delta_{kl} + (2/15)\sum_\alpha M_{\alpha,ij}M_{\alpha,kl} = (1/9)\delta_{ij}\delta_{kl} + (2/15)P_{ij,kl} \tag{B14}$$

When (B14) is combined with (B3), we obtain (2.29).

(37) M. Lax, "Symmetry Principles in Solid State and Molecular Physics", Wiley, New York, 1974.